

An Energy Dissipative Constitutive Model for Multi-Surface Interfaces at Weld Defect Sites in Ultrasonic Consolidation

Nachiket Patil, Deepankar Pal and Brent E. Stucker
Industrial Engineering, University of Louisville, KY 40292

A new finite element based constitutive model has been developed for quantification of energy dissipation due to friction and plastic deformation at the mating interface of two surfaces during the Ultrasonic Consolidation process. This work will include bridging the mesoscopic response of a dislocation density based crystal plasticity finite element framework at inter and intra-granular scales and a point at the macroscopic scale. This response will be used to develop an energy dissipative constitutive model for multi-surface interfaces at the macroscopic scale. The constitutive model will be used for quantification of energy consumed at lack of fusion and trapped oxide defects present in the build and the amount of energy input required to compensate for it. This numerical procedure will help in real time optimization of process parameters and closed loop control.

Introduction

Metal based additive manufacturing processes include both thermally-induced fusion processes and solid state processes. Some of the benefits of a solid state process lie in unique microstructures made possible because of near room temperature processing and the avoidance of solidification cooling induced residual stresses in the built part. These benefits can be further exploited if closed loop control of these processes becomes possible. The major hurdle in this is the computational complexity of the contact simulations, especially at the defect sites and the layer interfaces, involved in solid state processes like Ultrasonic Consolidation (UC). The present work is focused on development of a novel framework for interface simulations with the capability to include friction and various large deformation, nonlocal and geometrical nonlinearities involved in metal deformation.

Ultrasonic Consolidation

Ultrasonic consolidation (UC) is a solid-state additive manufacturing process which combines ultrasonic metal welding and milling to produce three dimensional objects. The process uses the high frequency ultrasonic shearing vibration at low amplitude and a normal force to break the oxide layers between two foils and then bond them by bringing together two nascent foil surfaces. Figure 1 shows a schematic of the UC process. The weld quality achieved in the process is sensitive to machine parameters. This sensitivity calls for better optimization of machine parameters through well informed computer simulations.

The UC process involves nonlinear plasticity which is inherently multi scale in space as well as time. The nonlinear and nonlocal plasticity in the process is dependent on the rate of deformation as well as size effects. The phenomenon of acoustic softening during UC is governed by these complicated material behaviors along with rate dependent dislocation dynamics. Continuum plasticity can be used to model the average phenomenon involved but it cannot account for the grain fragmentations or grain structure evolutions, which are at the core of the process if the quality of the weld is in question. A computational framework involving dislocation density based crystal

plasticity [1,2] has been developed. The computational cost involved in these simulations can be high and thus further work is required to reduce it by an order of magnitude to make it fast enough to work with machines for online process control.

In the present work a novel framework for developing interfacial constitutive models is presented to evaluate the macroscopic response of interfaces for various surface roughness values and material properties along with homogenization of dislocation dynamics near interfacial regions.

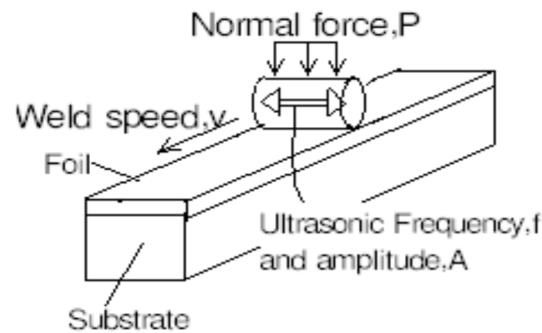


Figure 1: Schematic of UC process [1]

Interfacial Constitutive Model

The concept of an interfacial constitutive model has been researched for various applications like crack growth and propagation. The cohesive zone model [3,4] is considered as one of the pioneering interfacial constitutive models. The concept of a cohesive zone model can be further improved to simulate continuum level constitutive modeling of interfacial friction and sliding behavior [5]. Interfacial constitutive model literature is discussed in this subsection because it is closely related to the new formulation attempted in this work. The Extended Finite Element (XFEM) [6] methodology recently employed for multi-material and discontinuity simulations is another important development which has the capability to deal with various jump conditions involved at material interfaces. XFEM deals with discontinuities by decoupling a macroscopic average problem from the discontinuity problem at the FEM point integration level in order to calculate its effect on the stiffness matrices and macroscopic unbalanced forces. The decoupling of two problems rely on the functional evaluation of the coupling between the average macroscopic problem and the discontinuous behavior which could be a multi-scale phenomenon.

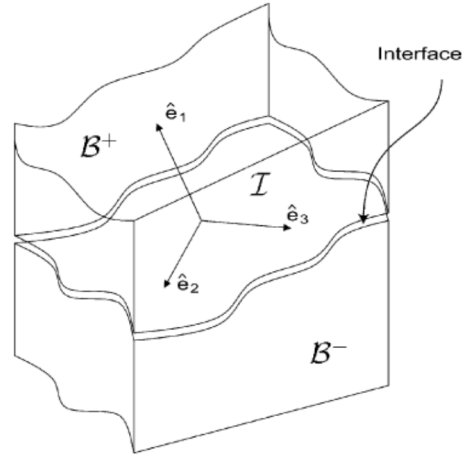


Figure 2: Interface between two bodies [5]

A cohesive interface between two bodies as shown in figure 2 can be describes as a contact interface between two bodies with or without any bonding mechanisms present at the interface. A constitutive model [5] for such an interface was developed by Su et. al and is discussed here to consider its potential application to Ultrasonic Consolidation. Consider two bodies β^+ and β^- separated by an interface \mathfrak{I} . Assume $\{\hat{e}_1, \hat{e}_2, \hat{e}_3\}$ is an orthonormal triad. The basis \hat{e}_1 is aligned with the normal \mathbf{n} to the interface, and $\{\hat{e}_2, \hat{e}_3\}$ are in the tangent plane at any point \vec{x} in the plane.

Let δ denote the displacement jump across the cohesive surface, and \mathbf{t} the power conjugate traction, such that $\mathbf{t}\dot{\delta}$ gives the power per unit of the interface in the reference configuration. The displacement jump can be decomposed into plastic and elastic deformation as follows.

$$\delta = \delta_e + \delta_p \quad (1)$$

The applied power per unit area of the interface can be denoted by

$$t\dot{\delta} = t\dot{\delta}_e + t\dot{\delta}_p \quad (2)$$

Let φ denotes the free energy per unit surface area in the reference configuration. The dissipation per unit area can be written as follows.

$$\Gamma = t\dot{\delta}_e + t\dot{\delta}_p - \dot{\varphi} \quad (3)$$

Plastic deformation produces no stresses. This leads to

$$t = K(\delta - \delta_p) \quad (4)$$

The yield surface for the interface point can be described as the intersection of two convex surfaces corresponding to normal mechanism (Φ_1) and shear mechanism (Φ_2) respectively as shown in figure 3.

$$\Phi_1 = t_N - s^1 \leq 0 \quad (5)$$

$$\Phi_2 = \bar{\tau} + \mu t_N - s^2 \leq 0$$

The evolution of plastic deformation is described mathematically as

$$\dot{\delta}_p = \sum_{i=1}^2 v^i m^i \quad (6)$$

$$m^1 = n$$

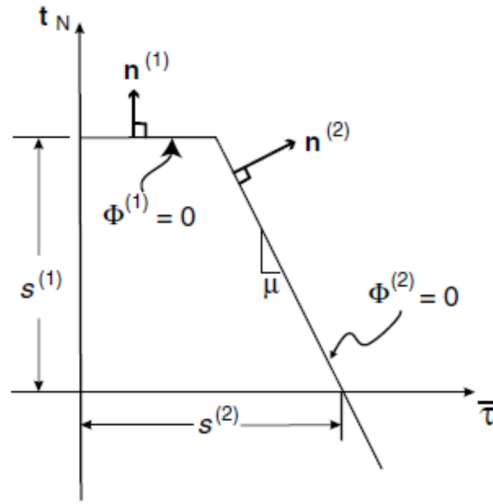


Figure 3: Schematic of the yield surface for normal and shear mechanisms [5].

$$m^2 = \frac{t_T}{\bar{\tau}} \quad (7)$$

This is a non-normal flow rule for the shear response. Finally the required consistency condition for plastic deformation is as follows.

$$v^i \Phi_i = 0, \text{ when } \Phi_i = 0 \quad (8)$$

The consistency equation helps identify the possibility of plastic deformation. The magnitude of plastic deformation has to be further determined based on the evolution of s^i as a function of time. The evolution mechanisms for s^i are in general described as hardening and softening and their evolution is a function of dislocation dynamics; and a detailed crystal plasticity simulation is required in order to capture them for general loading and geometry scenarios with given macrostructure information on both sides of the interface.

Applications of the interfacial constitutive models

The interfacial constitutive law will help in simulation of the process at the macroscopic scale, which will result in reduced computational complexity. Other applications for such a model include engineering problems such as cohesive modeling of crack interfaces during their propagation. The contact problem is also significant from the perspective of bonded or unbonded joints in metals. These energy dissipation laws will be also helpful in developing constitutive models and new interfacial elements for macroscopic vibration simulations.

The application of such an interfacial model in additive manufacturing other than UC process will include support snapping simulation for Selective Laser Melting (SLM) process where an initial crack in the lattice will grow and cause support structures failure. In case of SLM delamination possibility of two successive layers built with significant recoat time can be also studied in depth. The friction stir surfacing process can be also modelled efficiently with the proposed simulation framework.

Mathematical Formulation

Finite Element Formulation

The schematic problem description is given in figure 4. Simple 3D brick elements are used for FEM simulation.

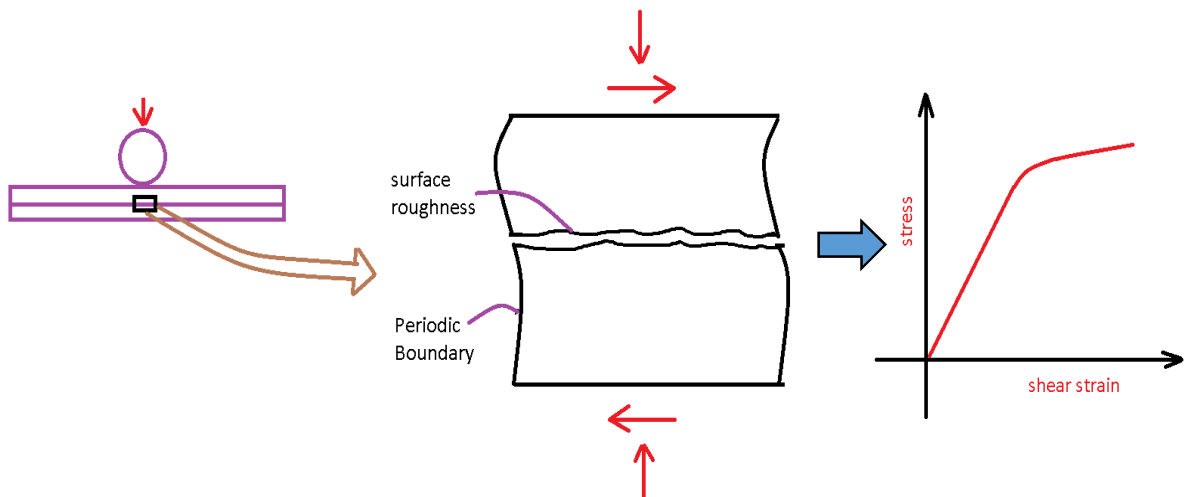


Figure 4: Schematic diagram presenting the concept of an interfacial constitutive model for a macroscopic interface contact

The virtual work equation is written in virtual work formulation as

$$\delta V = \int (\delta \varepsilon) C(\varepsilon) dv + \delta W(\delta u) = 0 \quad (9)$$

$$\varepsilon = [B]\mathbf{q} \quad (10)$$

The \mathbf{q} vector is the nodal displacement vector. The equation above leads to the element stiffness equation which is

$$K_{elem} = B^T C B \quad (11)$$

The nodal equilibrium in the global coordinate system will lead to a final finite element equation which is

$$[K_{global}]\mathbf{u} = \mathbf{F}_{global} \quad (12)$$

The traditional approach to assemble a stiffness matrix from local to global coordinate systems is of individually substituting each value in the K_{elem} into K_{global} . The present work includes development of a new mapping from local to global coordinate systems which will simplify the FEM assembly process in the case of contact problems where connectivity is updated as per the updated contact surface configuration.

$$[K_{global}] = Perm [K_{Local}] Perm^T \quad (13)$$

In case of changing contact surface configurations this can be modified as follows,

$$[K_{updated}] = Perm [K_0] Perm^T \quad (14)$$

where $[K_0]$ = (Stiffness Matrix) without any contact constraints, $Perm$ = (Transformation matrix) which maps one configuration to another and has the following mathematical form, where R is a mathematical relation or a second order tensor.

$$Perm = ARB \quad (15)$$

Where A is a set of all nodes in the initial configuration and B a set of nodes in the final configuration.

The forces also follow a similar map as follows.

$$[F_{updated}] = Perm[F_0] \quad (16)$$

Contact Surface Constraints and solution of constrained simultaneous equations

1.0 Slave Nodes

The contact surface constraints are based on the gap function to evaluate contact which is defined as

$$\mathbf{g}(x, y) = u_{t3}(x, y) - u_{b3}(x, y) \quad (17)$$

where $u_{t3}(x, y)$ is the z-direction displacement of the top surface at point (x,y). Similarly $u_{b3}(x, y)$ stands for the bottom surface. If the $\mathbf{g}(x, y) = 0$ and shear is less than the friction resistance, then the top surface node is treated as a slave to the bottom surface. This is achieved by providing a constraint based on the shape functions of the bottom surface element as follows:

$$q_t = N_1q_1 + N_2q_2 + N_3q_3 + N_4q_4 \quad (18)$$

where q_t is any x, y or z displacement of a node on the top surface and q_i are corresponding displacements on the bottom target element.

The constraint equations are solved by splitting the slave node stiffness matrix row into different rows. Each split row will be added to the master Degree of Freedom (DOF) row based on the N_i in the constraint equation for the master DOF. This methodology is explained in figure 5.

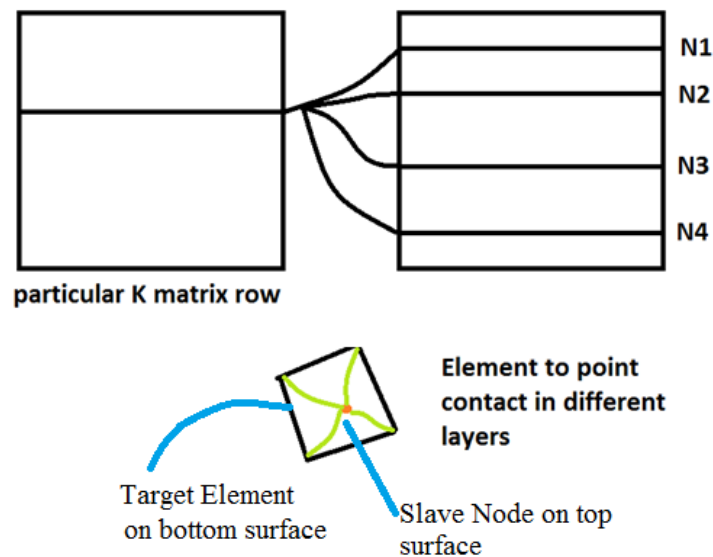


Figure 5: Schematic diagram representing a slave node constraint on a contact surface and its solution methodology by splitting slave node stiffness as per the constraint equation.

2.0 Free Nodes

A DOF is set free if it is sliding or has lost contact with the bottom surface.

3.0 ($g(x, y) \leq 0$) condition

To simplify the algorithm, top surface nodes that are impinging are first allowed to impinge and then are forced back to the bottom surface iteratively.

Contact Simulation Algorithm

The contact simulation algorithm is based on minimizing unbalanced force iteratively along with updated contact constraints. First contact constraints are updated which will induce some unbalance forces due to shear slip and change in stiffness. These unbalanced forces are solved in the new configuration which can further change the gap function and can change the contact constraints. The algorithm is presented in a flow chart format in figure 6.

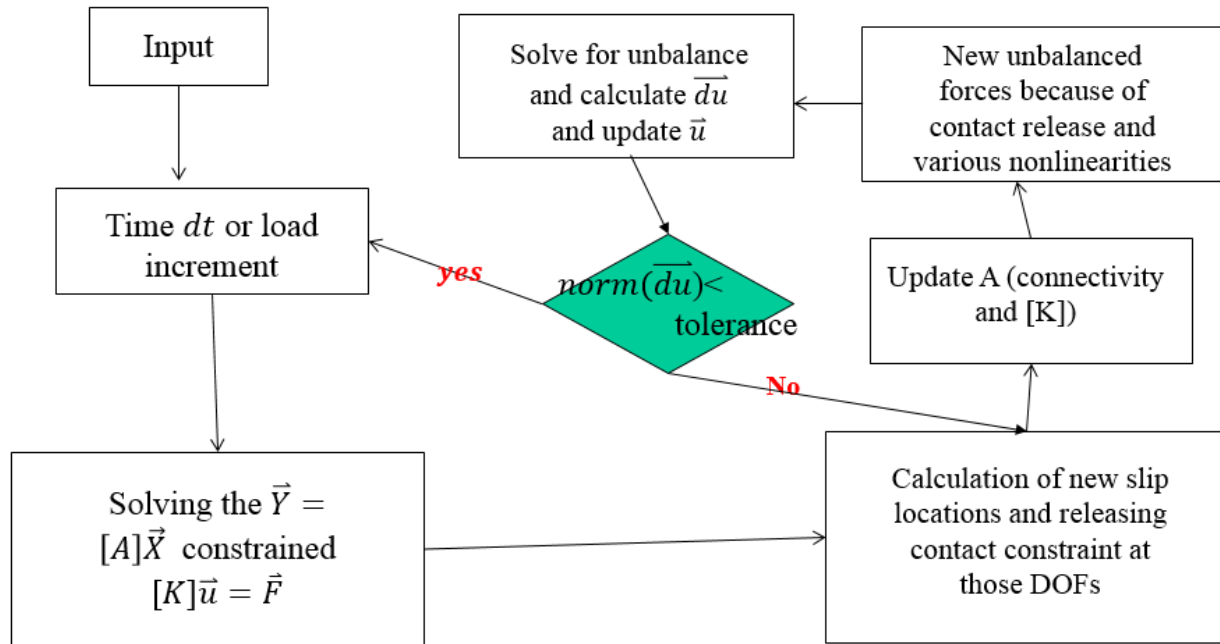


Figure 6: Flow chart showing FEM algorithm used for contact simulation

Case Study

A simple case of surface to surface contact is considered here. Two prismatic blocks of size $0.001 \times 0.001 \times 0.0005 \text{ m}^3$ are in contact with each other as shown in figure 7. The z-direction height of each block is 0.0005m. The boundary conditions include a bottom surface fixed in all degrees of freedom and a top surface with slip and normal compressive displacement boundary conditions as shown in figure 7. The details of the boundary conditions and material properties are as follows.

Top Surface:

$$u_1(x, y) = \text{slip}(t)$$

$$u_2(x, y) = 0$$

$$u_3(x, y) = -0.00001\text{m}$$

Bottom Surface:

$$u_1(x, y) = 0$$

$$u_2(x, y) = 0$$

$$u_3(x, y) = 0$$

Sides: No constraint

Material Properties: Linear elastic

$$E = 2 \times 10^{11} \text{N/m}^2$$

$$\mu = \text{poisons ratio} = 0.3$$

$$\text{Friction coefficient} = 0.3$$

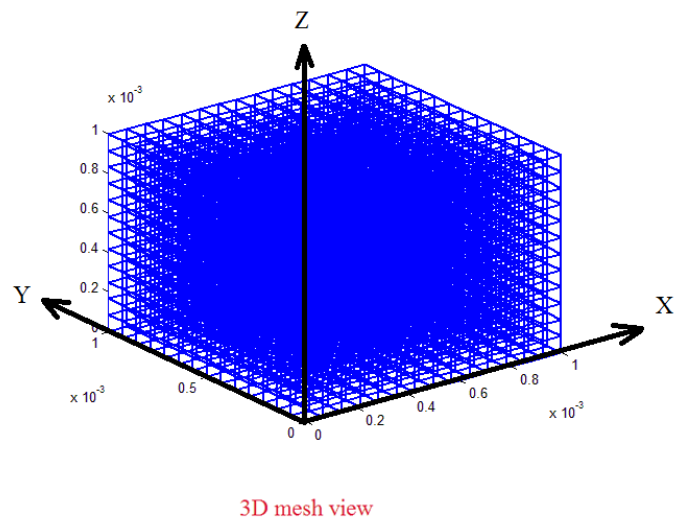
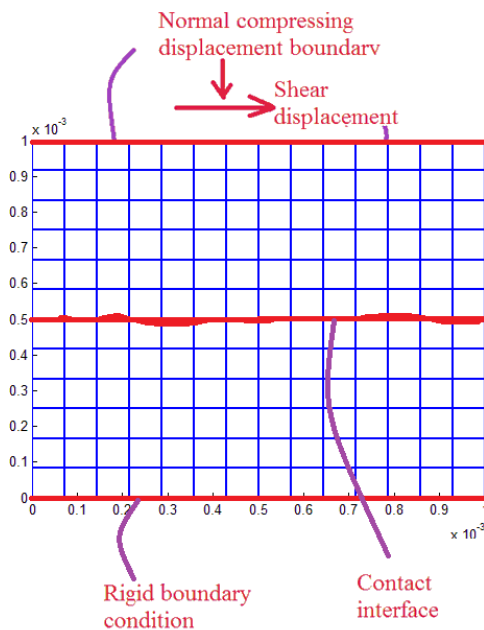


Figure 7: Problem geometry and boundary conditions

Results and Discussion

The present work is a small case study to verify whether future work deriving interfacial constitutive models is merited. The correct boundary conditions for extracting constitutive models are outside the focus of this work, as this work focused on formulating a FEM framework which can consider different boundary conditions and give high fidelity contact simulations. The parameters of interest in this case study are the macroscopic aggregate shear resistance and macroscopic strain.

The shear resistance of the contact surface is defined below. Considering the prismatic geometry of the model the total shear resistance for any cross-section will come out to be same.

$$\text{Aggregate Shear Force} = S = \int^{c/s \text{ area}} (\sigma_{13}) ds \quad (19)$$
$$\text{Aggregate Normal Force} = N = \int^{c/s \text{ area}} (\sigma_{33}) ds$$

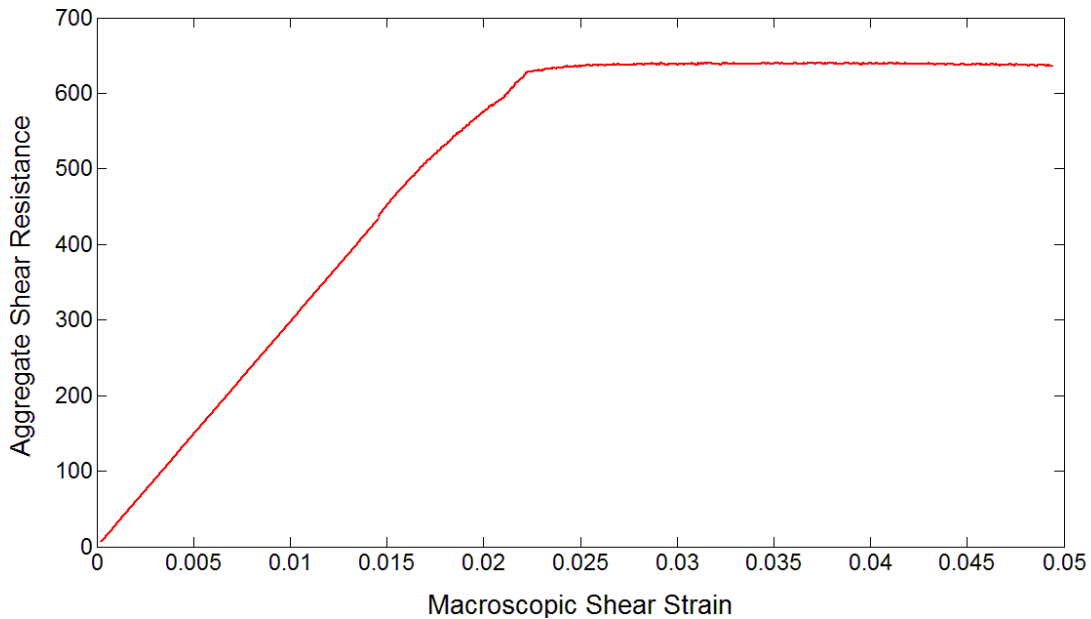


Figure 8: Macroscopic strain versus shear resistance plot

The plot of S versus slip given at the top surface is shown in figure 8. The reason behind the fall of the shear resistance with increase in slip is due to contact being lost at the extreme left or right points due to the overhanging nodes at the end. Figure 9 shows a plot of macroscopic friction coefficient calculated as a ratio of S and N at each time instant during slip loading in the simulation. The reason for a macroscopic friction coefficient less than 0.3 of that of the actual interface can be attributed to the fact that the shear resistance at each point in the cross-section is not utilized

completely in one particular configuration or point in the time. Another way to explain it is that the 0.3 is the maximum upper bound that can be achieved.

The shear resistance will be totally lost at the overhangs because there is no material available on either side for contact friction as seen in the deformed shape shown in figure 10.

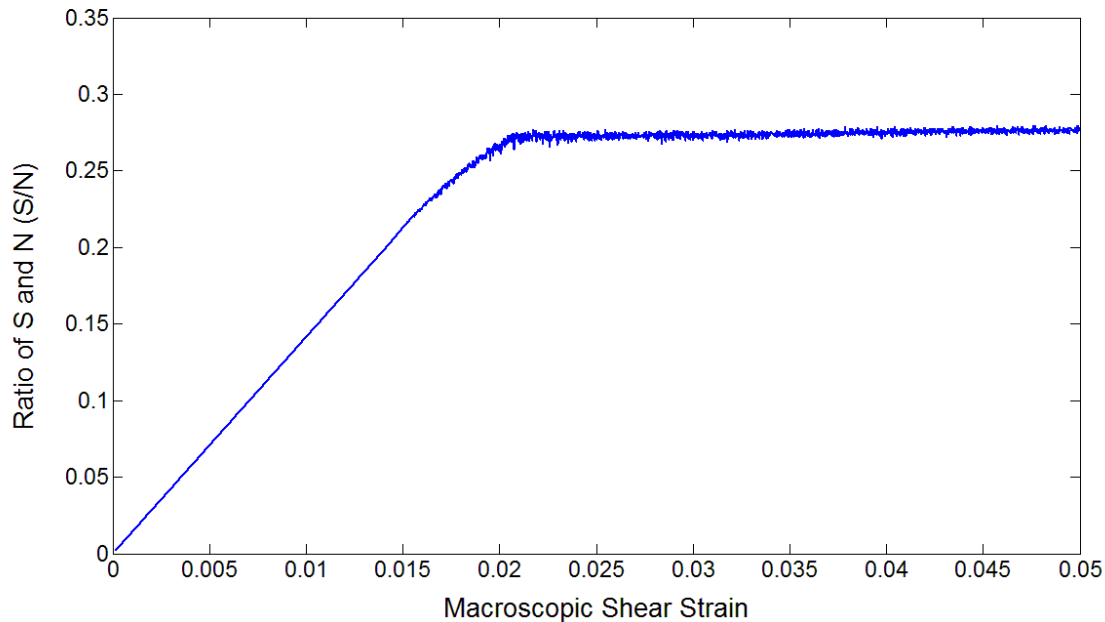


Figure 9: Plot of the macroscopic friction coefficient

Conclusions and future work

A novel framework for an interfacial friction model has been developed in the present work. The developed contact simulation framework shows good behavior at the contact interface. The novel features of this framework include:

- Mathematical framework for efficient assembly of FEM matrices
- Solution of constraint equations exactly without any additional computational cost
- No addition of penalty springs which can introduce spurious stiffening behavior at interface

The future work in this problem will include addition of the following features to the present framework in order to develop interfacial constitutive models or laws:

- Nonlinear simulations with crystal plasticity based material constitutive models for metals.
- Inclusion of tangent stiffness at the current configuration (Geometric nonlinearity)
- Periodic boundary condition considering the case of deriving a constitutive model for a point on an interfacial surface.
- Inclusion of surface roughness

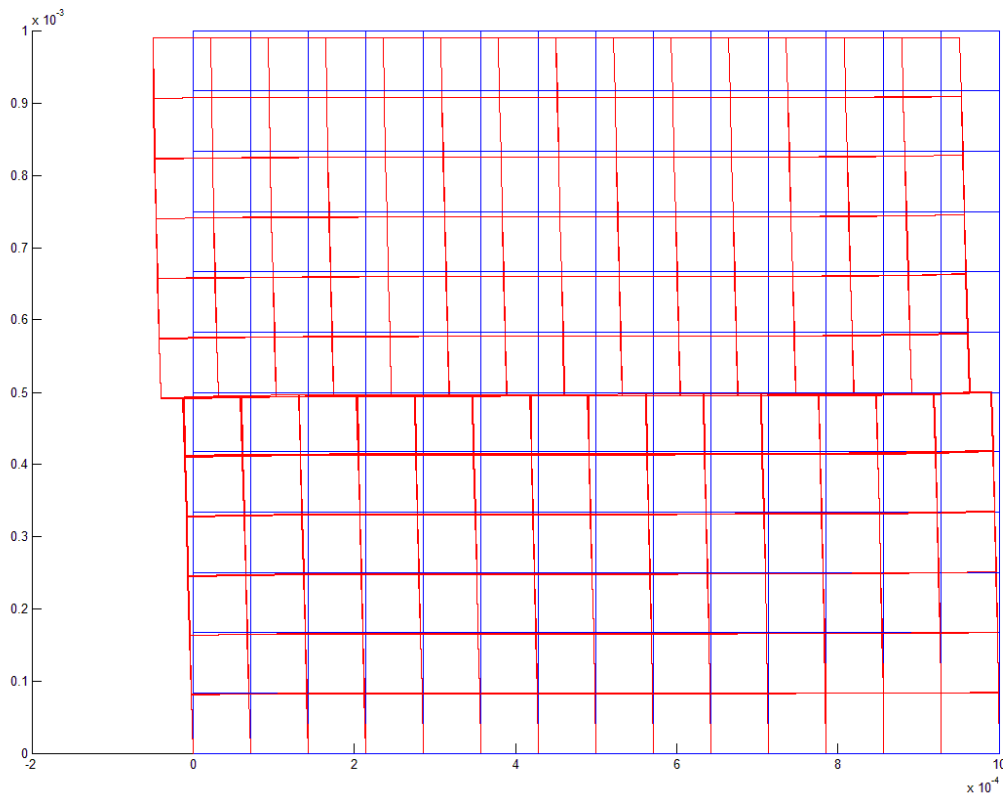


Figure 10: Deformed and un-deformed mesh at a macroscopic shear strain of 0.05

Acknowledgements

The authors would like to acknowledge the Office of Naval Research (ONR) for support through Grant No. N00014-11-1-0689.

References

-
- [1] Pal, D., (2011), Dislocation Density-Based Finite Element Method Modeling of Ultrasonic Consolidation, PhD thesis, Utah State University, Logan, Utah.
 - [2] Pal, D., Patil, N., & Stucker, B. (2013). A study of subgrain formation in Al 3003 H-18 foils undergoing ultrasonic additive manufacturing using a dislocation density based crystal plasticity finite element framework. *Journal of Applied Physics*, 113, 203517.
 - [3] Barenblatt, G. I., (1962). The mathematical theory of equilibrium cracks in brittle fracture, *Advances in Applied Mechanics*, 7(1), 55-129.

[4] Dugdale, D. (1960). Yielding of steel sheets containing slits. *Journal of the Mechanics and Physics of Solids*, 8(2), 100-104.

[5] Su, C., Wei, Y.J., & Anand, L., (2004), An elastic–plastic interface constitutive model: application to adhesive joints, *International Journal of Plasticity* 20(12), 2063–2081.

[6] Dolbow, J. O. H. N., & Belytschko, T. (1999). A finite element method for crack growth without remeshing. *Int. J. Numer. Meth. Engng*, 46, 131-150.